Effect of Die-upset Process on Magnetic Properties and Deformation Behavior of Nanostructured Nd-Fe-B Magnets

R. Zhao, W. C. Zhang, J. J. Li, H. J. Wang, M. G. Zhu, and W. Li*

Division of Functional Materials, Central Iron & Steel Research Institute, Beijing 100081, China

Nd-Fe-B high performance magnets were prepared by die-upset forging. The effects of the deformation parameters on magnetic properties and flow stress were studied. Deformation temperatures in the range of 600~900 °C enable to achieve an effective anisotropy and temperature 800 °C proves to be suitable for deformation of Nd-Fe-B magnets. The amount of c-axis alignment along the press direction seems to depend on the amount of deformation and a saturation behavior is shown at deformation ratio of 75%. Magnetic properties are also related to strain rate, and maximum energy product is attained at an optimum strain rate of $\dot{\phi} = 1 \times 10^{-2}$ s^{-1}. By analyzing the relationship of stress and strain at different deformation temperature during die-upset forging process, deformation behavior of Nd-Fe-B magnets was studied and parameters for describing plastic deformation were obtained. Nd-rich boundary liquid phase, which is additionally decreasing the flow stress during deformation, is supposed to play the role of diffusion path and enhance the diffusion rate.

Keywords : Nd-Fe-B magnet, die-upset, strain rate, deformation ratio, plastic deformation

1. Introduction

Fully dense, anisotropic Nd-Fe-B magnets with excellent magnetic properties can be produced by melt spinning, followed by hot pressing and subsequent die-upsetting. The maximum energy product is up to 54.4 MGOe [1-3]. The optimally quenched melt-spun ribbons have equiaxed and randomly oriented $Nd_2Fe_{14}B$ grains. Hot pressing of ribbon powder achieves complete densification and a desired shape while maintaining essentially an isotropic structure and magnetic properties. The subsequent hot deformation process modifies the equiaxed grains to platelets with increasing in grain size. The mechanism of anisotropic formation has been suggested to be a combination of grain boundary sliding and anisotropic grain growth in a direction normal to the applied stress [4-7]. An extensive study was also carried out by Grünberger *et al.* [8], in which he suggested a dominating role of the diffusion creep mechanism accompanied by rheological and viscous flow. The deformation process of nanostructured magnets which can be interpreted by the model of solution-precipitation creep plays an important role in

the formation of microstructure and magnetic anisotropy. Therefore the research in deformation process and deformation mechanism could help us to understand the hot formability of the magnets and the microstructural mechanism of both hot deformation and texturing. It is beneficial to obtain the best hot deformation conditions (also tool design) and the technological limits for a crack-free production of magnets with maximum texture and optimum magnetic properties.

In this study hot deformation parameters included deformation temperature, strain rate and deformation ratio has been studied for Nd-Fe-B die-upset magnets. Magnetic measurements, X-ray diffraction and field emission scanning electron microscope were applied for the study of magnetic properties and crystallographic alignment for the specimens subjected to different deformation conditions. The analysis of experimental kinetic data was based on the model of solution-precipitation creep.

2. Experiment

Melt-spun powder ($Nd_{30}Fe_{64.55}Co_4B_{0.95}Ga_{0.5}$) were hot pressed in vacuum at 550 °C, by applying a pressure of 113 MPa to samples with a diameter of 13 mm and a height of $h_0 = 27$ mm. The die-upsetting experiments were

---

*Corresponding author: Tel: +86-10-62185125
Fax: +86-10-62182610, e-mail: magnet@cisri.com.cn

performed under an argon atmosphere at temperature from 600 °C to 900 °C with strain rates from 10^{-3} to 10^{-1} s^{-1}. The flow stress was measured at constant strain rate as a function of strain $\varphi = \ln(h_0/h)$ with h_0 as the starting height of the sample and h the height after deformation. Specimens were cut from the center of magnets and the magnetic properties were measured parallel to the pressing direction, using NIM2000 hysteresisgraph. Texture distribution in pressure direction was determined by X-ray diffraction. Microstructure investigations were performed on specimens parallel to the deformation direction by HRSEM.

3. Results and Discussion

3.1. Effect of deformation temperature on magnetic properties

The effect of deformation temperature on the magnetic properties is shown in Fig. 1. The temperature 800 °C proved to be most suitable for deformation of Nd-Fe-B magnets and produced high performance magnetic properties. At a low temperature, the amount of non-favorably oriented crystalline which is dissolved in liquid phase decreases and the fluidity of Nd-rich liquid phase becomes poor. So c-axis alignment cannot comparable to the case of optimal temperature and it may be responsible for the low remanence and low maximum energy product. On the other hand, a higher temperature such as 900 °C can lead to grain coarsening and prevent anisotropically grown fine grains from grain boundary sliding and rotation, which results in deterioration of the remanence and
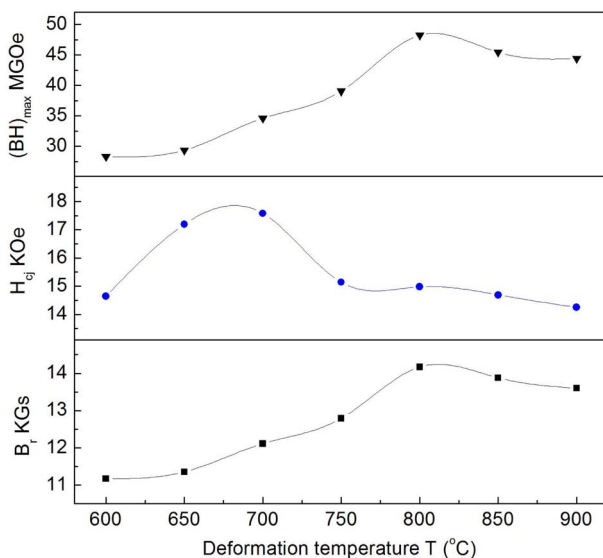
Fig. 1. (Color online) The effect of deformation temperature on the magnetic properties of die-upset magnets.
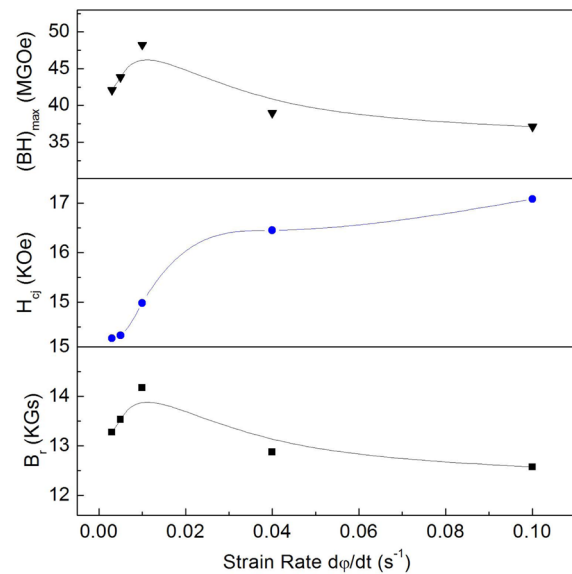
Fig. 2. (Color online) The effect of strain rate on the magnetic properties of die-upset magnets.

substantial decrease of the coercivity. The deformation temperature 800 °C produces optimum microstructure giving high remanence and maximum energy product of 14.17 KGs and 48.23 MGOe respectively.

3.2. Effect of strain rate on magnetic properties

Fig. 2 shows the strain rate dependence of magnetic properties and suggests that there is an optimum strain rate existing to obtain higher remanence. However, coercivity increases monotonously with strain rate. Since coercivity is dependent on grain size [9], as the result of a longer deformation process at a lower strain rate, a lower coercivity is caused by grain coarsening. This also leads to lower remanence since the coarse grains prevent anisotropically grown fine grains from alignment. The higher strain rate does not allow enough time for anisotropic c-plane grain growth essential for crystallographic alignment.
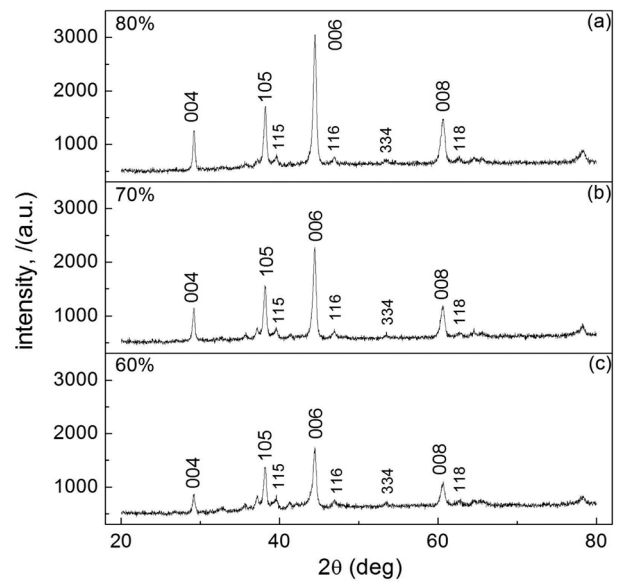
3.3. Effect of deformation ratio on magnetic properties

The remanence is slightly enhanced in press direction up to values above 9.4 KGs already after the hot compaction and it increases with the degree of deformation. Fig. 3 shows the remanence B_r in press direction as a function of the deformation ratio for a deformation temperature T = 850 °C and strain rate $\dot{\varphi} = 5 \times 10^{-3}$ s^{-1}. At higher deformation ratio the enhancement of remanence is slow, indicating a saturation behavior. The optimum magnetic property appears at deformation ratio of 80%. Due to the inhomogeneous flow during deformation, micro-
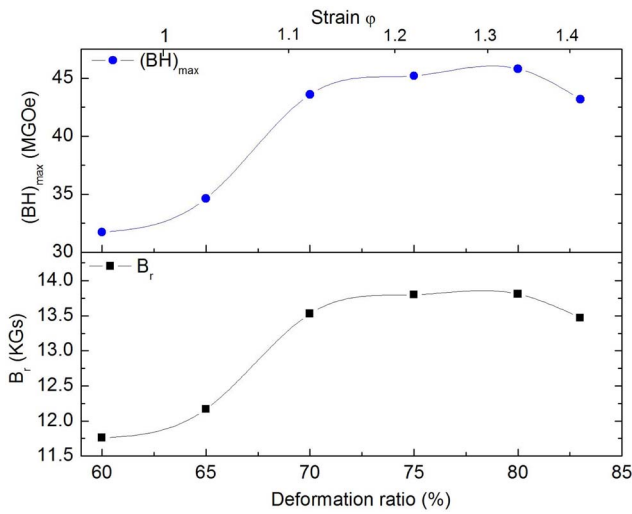
Fig. 3. (Color online) The effect of deformation ratio on the magnetic properties of the die-upset magnets.

Fig. 4. The XRD patterns of die-upset magnet specimens with different deformation ratio: (a) 80% (b) 70% (c) 60%.

structure and magnetic properties are not homogeneous distributed in the magnet. It seems that the optimal performance only concentrates in the central region of die-upset magnet [10]. In order to exclude the influence of such inhomogeneity, die-upset magnets must be prepared in the same height at the end of deformation and a small cylinder sample is cut from the central region to be used for magnetic measurement. For the restriction of die size, the height of die-upset magnet reduced with the increase of deformation ratio. Therefore after reaching a certain deformation ratio it is difficult to enhance magnetic properties still by increasing the deformation ratio. The magnetic properties of highly die-upset Nd-Fe-B magnets are limited by nonuniform deformation. Furthermore, high deformation ratio also leads to formation of deformation defects, such as the microcracks between melt-spun flakes in the magnet, which lower the magnet's density and remanence. As shown in Fig. 3, when defor-

mation ratio reached 80%, magnetic properties began to deteriorate.

Fig. 4 shows the XRD patterns of magnets with different deformation ratio. Texture can be evaluated by the relative intensity ratio of the (006) peak to (105) peak as shown in Fig. 4. High ratios are generally associated with optimum grain alignment. The ratio of the (006) to (105) peaks was calculated to be 1.26, 1.45 and 1.78 for the deformation ratio 60%, 70% and 80% respectively. With the increasing of deformation ratio, a better crystal alignment is obtained and leading to a higher remanence and maximum energy product.

Crystallographic and magnetic anisotropy is introduced in the material in the course of die-upset forging. The magnetic properties depend on the microstructure of the material. HRSEM micrographs of fractured surfaces show
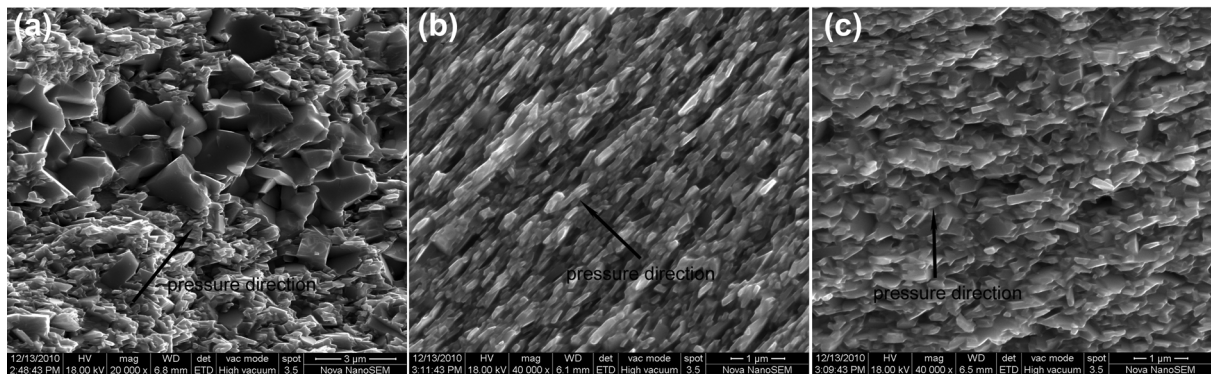
Fig. 5. HRSEM micrograph of the fractured surface of die-upset forged magnets, deformed at 850 with different deformation ratio: (a) 60% (b) 70% (c) 83%. The pressure direction is indicated.
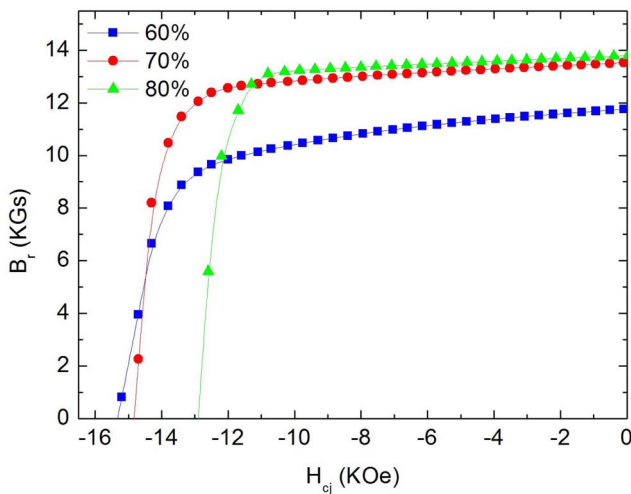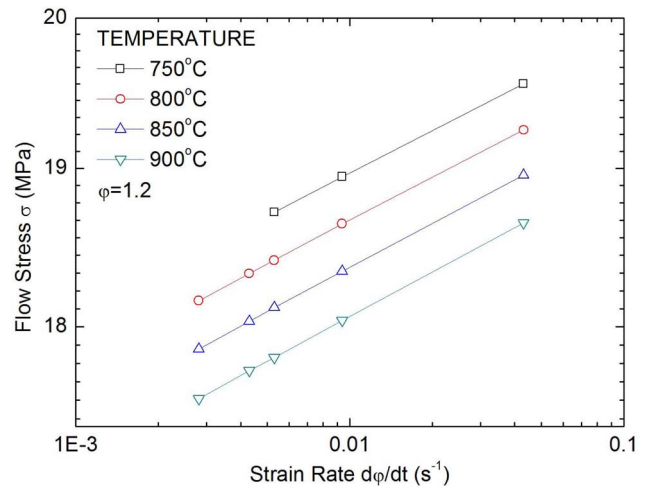
Fig. 6. (Color online) Demagnetization curves for die-upset magnet specimens with deformation ratio 60%, 70% and 80%.
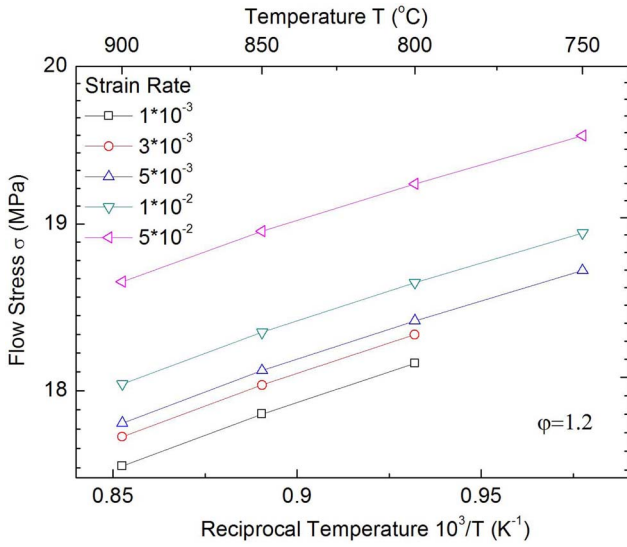

Fig. 7. (Color online) Relationship between flow stress and strain rate after deformation at different temperature. The stress exponent amounts to n = 2.5.

the expected platelet-shaped grains with their flat surfaces perpendicular to the upset direction. Fig. 5 shows the microstructure of magnets, which were die-upset forged at 850 °C with 60%, 75% and 83% deformation and the pressure direction is indicated in it. In Fig. 5(a), the case of 60% deformation ratio, the visible growth of regions with equiaxed coarse grains (with grain sizes in the order of 2 μm) which start from flake boundaries is noteworthy. The size distribution is also very broad. It supposed that the compaction and deformation process with low reduction ratio in height produce defect-rich regions at the contacts between the flakes which are starting points of the coarsening analogous to the case of highly die-upset. The existence of very large grains and poor alignment are responsible for the low magnetic properties. Greater deformation, 75%, at 850 °C, produces much better alignment and magnetic properties. This is evidenced from the microstructure as shown in Fig. 5(b) and has also confirmed the results of X-ray diffraction shown in Fig. 4. For deformation ratio of 83%, poor crystallographic alignment is shown in Fig. 5(c), which may lead to the deterioration of magnetic properties.

Hysteresis loops for die-upset magnets with deformation ratio 60%, 70% and 80% are shown in Fig. 6. Die-upset ratio changes the substantial shape of the demagnetization curves. We can see that die-upset with increasing deformation ratio leads to a decrease of the coercivity and a substantial increase of the remanence. Moreover, the curve shape becomes more square, which contributes to the $(BH)_{max}$ increase.

3.4. Hot deformation behavior of nanostructured Nd-Fe-B magnets

Deformation process determines the final performance of die-upset magnets. Thus the research of deformation mechanism can contribute to understand the influence of the grain boundary phase, the development of microstructure and texture as well as the magnetic properties. All the creep models lead to the following general equation

$$\dot{\varphi} = A\sigma^n \exp\left(-\frac{Q}{RT}\right) \qquad (1)$$

where $\dot{\varphi}$ is the strain rate, A a microstructure-dependent quantity, σ the flow stress, n the stress exponent, Q the effective activation energy of the process, R the molar gas constant, and T is the absolute temperature. Here we will consider the models of solution-precipitation creep because of the existence of a liquid grain-boundary phase. The fundamental assumption is corresponding with classic creep models of Nabarro-Herring and Coble which describe diffusion-controlled transport through the grains and along the grain boundaries in elastically stressed single-phase systems.

Fig. 7 shows the dependence of flow stress on strain rate at $\varphi = 1.2$ and with different temperature. The linearly fitted curves on a double logarithmic scale are parallel and reveal a power law $\dot{\varphi} \propto \sigma^n$ with a stress exponent $n \approx 2.5$ which can describe the deformation behavior. Fig. 8 shows the flow stress versus the reciprocal deformation temperature at $\varphi = 1.2$ and different values of $\dot{\varphi}$. The approximation by straight lines indicates a thermally activated process through the complete range of deformation temperature which can be obtained by an Arrhenius' plotting of flow stress versus deformation temperature following the equation

Fig. 8. (Color online) Relationship between flow stress and temperature for different strain rate at the same strain indicating a uniform thermally activated process.

$$\ln \sigma = \frac{a}{T} + b \qquad (2)$$

By applying logarithm on both sides of creep model equation we can obtain the equation

$$\ln \sigma = \frac{1}{n} \cdot \frac{Q}{RT} + \frac{1}{n}(\ln \dot{\varphi} - \ln A) \qquad (3)$$

Comparing the two equations (2) and (3) above, it is obvious that $a = 1/n \cdot Q/T$ and $b = 1/n(\ln \dot{\varphi} - \ln A)$. Stress exponent n is taken as the value of 2.5 and strain rate $\dot{\varphi}$ is known as an experimental default parameter, the values of slope a and intercept b can be obtained in Fig. 7. Calculation results indicate that activation energy and the constant amount to $Q = 152$ KJ/mol and $A = 1 \times 10^{-14}$ respectively. Such calculation results will be used as default parameters in the finite-element simulations to study the inherent inhomogeneity of the deformation process in future research.

As shown in Fig. 6 and Fig. 7, flow stress increases with the decreasing of deformation temperature and with the increasing of strain rate. The decreasing of deformation temperature or increasing of strain rate which leads to a shorter exposure time at high temperatures can effectively inhibit grain coarsening and growing up and is beneficial for the improvement of microstructure. Comparing with the case of high deformation temperature and low strain rate, however, there is little grain boundary phase existing in the liquid state. So it is much more difficult to complete the plastic deformation process due to the increase of diffusion activation energy and a larger flow stress is

needed. This indicates the important role of liquid grain boundary phase which enables rapid grain boundary sliding and grain growth by enhancing the diffusion rate. Furthermore, the anisotropic growth of grains induced by external stresses is at the expense of adjacent grains [11]. So the main part of the deformation is a result of stress-induced anisotropic grain growth and a combination of grain boundary sliding and rotation which is facilitated by grain boundary liquid phase. The value of n = 2.5 also confirms that grain boundary sliding is occurring during deformation [12].

4. Conclusion

The effects of the deformation parameters of the die-upsetting procedures on magnetic properties and flow stress were studied. The analysis of the stress strain-rate relations for die-upsetting experiments in a deformation temperature range from 600 °C to 900 °C yields a stress exponent n = 2.5 for activation energy of Q = 152 KJ/mol and a constant of A = 1×10^{-14}. The grain boundary phase in the liquid state acts as lubricant between the grains and particularly between the melt-spun flakes, additionally decreasing the flow stress during deformation. Deformation temperatures in the range of 600-900 °C enable to achieve an effective anisotropy, however, much higher and much lower temperatures produce lower remanence and lower maximum energy product. The amount of c-axis alignment along the press direction seems to depend on the amount of deformation and a saturation behavior is shown at deformation ratio of 75%. Magnetic properties are also related to strain rate, and maximum energy product is attained at an optimum strain rate of $\dot{\varphi} = 1 \times 10^{-2}$ s^{-1}.

Acknowledgements

References

[1] T. Saito, M. Fujita, T. Kuji, K. Fukuoka, and Y. Syono, J. Appl. Phys. **83**, 6390 (1998).
[2] P. P. Yi, D. Lee, and A. R. Yan, J. Magn. Magn. Mater. **322**, 3019 (2010).
[3] L. Wojciech and H. A. Davies, J. Alloys Compd. **491**, 694 (2010).
[4] L. Li and C. D. Graham, IEEE Trans. Magn. **28**, 2130 (1992).

[5] A. Kirchner, J. Thomas, O. Gutfleisch, D. Hinz, K.-H. Müller, and L. Schultz, J. Alloys Compd. **365**, 286 (2004).

[6] A. H. Li, W. Li, B. Lai, H. J. Wang, M. G. Zhu, and W. Pan, J. Appl. Phys. **107**, 09A725 (2010).

[7] D. N. Brown, B. Smith, B. M. Ma, and P. Campbell, IEEE Trans. Magn. **40**, 2895 (2004).

[8] W. Grünberger, D. Hinz, A. Kirchner, K.-H. Müller, and L. Schultz, J. Alloys Compd. **257**, 293 (1997).

[9] H. T. Kim, Y. B. Kim, G. A. Kapustin, W. Y. Jeon, and H. S. Kim, J. Magnetics **7**, 138 (2002).

[10] C. D. Fuerst and E. G. Brewer, J. Appl. Phys. **73**, 5751 (1993).

[11] H. W. Kwon and J. H. Yu, IEEE Trans. Magn. **45**, 4435 (2009).

[12] Y. Yoshida, Y. Kasai, T. Watanabe, and S. Shibata, J. Appl. Phys. **69**, 5841 (1991).